3D Beamforming Technologies and Field Trials in 5G Massive MIMO Systems

Jiangzhou Wang, *Fellow, IEEE,* Wei Deng, Xin Li, Huiling Zhu, Senior Member, IEEE, Manish Nair, Tao Chen, Senior Member, Na Yi, Member, IEEE, and Nathan Gomes, Senior Member, IEEE

(Invited Paper)

Abstract In this paper, three-dimensional (3D) beamforming characteristics and applications in fifth generation (5G) mobile communications have been studied by considering the physical structure of array antennas, and the properties of the 3D beam pattern formed by planar, rectangular array antennas. Array beam gains are formulated according to rectangular array antennas. The effect of array antenna configuration on 3D beamforming is studied especially according to the building height. The field trial and measurement results have been presented for single and multiple mobile users. The field trial results show that (1) The total sum rate from all users can be increased multiple times (i.e. 3 to 4 times) as large as that of a single user. When the number of users is larger than 8, the sum rate becomes saturated; (2) Users with uniform angular distribution can achieve larger sum rate than users with centralized distribution due to space separation; (3) The performance of the multi-antenna system is best under static-user conditions, with it dropping considerably for mobile conditions, even by more than 50% due to poor channel state information estimation; (4) In case of 3D beamforming, good coverage performance can be achieved in medium or high buildings.

***Index Terms*—5G, Massive MIMO, 3D beamforming, multiuser communications**

I. Introduction

Fifth generation (5G) mobile communication has been developing very rapidly. To meet the demand for high system capacity, effort has been made by scientists and researchers in the aspects of increasing the efficiency of existing resources and exploring newly available resources (e.g. the spatial domain) suitable for wireless communications. Investigations aiming to improve the efficiency of various resources (i.e. in time, frequency, and spatial domains) have attracted research interest for dozens of years, created abundant outcomes in both theory and application scenarios from single-user to multi-user systems; from single input single output to multiple input multiple output (MIMO) and further to massive MIMO [1]-[2]; from single mode to multiple mode system (i.e. time domain to space-time domain processing architecture) [3]; from orthogonal to non-orthogonal coding, modulation and estimation systems [4]-[6].

In particular, developing the spatial domain resource attracts worldwide research interest. Among this, research on beamforming technology is a hot topic [7]-[9]. The rapidly increasing challenges emerge among the scarcity of available resources, such as time, frequency spectrum and code that can be employed in wireless communications, and the dramatically increasing demand for higher data rate and system capacity, making spatial resource more important than ever in wireless communication systems.

Beamforming refers to the function of smart antennas which controls the properties of the electromagnetic wave radiation pattern of an array antenna by aligning the amplitude and phase of transmitting/receiving signals in the array antenna elements thus increasing the array antenna gain in the intended angle of direction, and at the same time, suppressing gain in other angular directions where interference signals would result. Beamforming can increase signal-to-interference-plus-noise ratio (SINR) for intended users, providing multiple benefits for the system, such as, higher system capacities, lower transmit power, and greater frequency reuse factor within a given area. In general, beamforming techniques encompass two types, switched-beam and adaptive beamforming systems.

Manuscript received 21 July 2020; revised 14 September 2020.

J. Wang, H Zhu, M Nair, and N Gomes are with the School of Engineering and Digital Arts, the University of Kent, CT2 7NT, UK (h.zhu@kent.ac.uk, m.nair@kent.ac.uk, n.j.gomes@kent.ac.uk,j.z.wang@kent.ac.uk)

W Deng and Xin Li are with China Mobile Research Institute, Beijing, China, (dengwei@chinamobile.com, Lixin@chinamobile.com)

T Chen is with VTT Technical Research Centre of Finland, Espoo, Finland, (tao.chen@vtt.fi)

N Yi is with University of Surrey, Surrey, GU2 7XH, UK (n.yi@surrey.ac.uk)

This article has been accepted for publication in a future issue of this journal, but has not been fully edited. Content may change prior to final publication. Citation information: DOI 10.1109/OJVT.2020.3030774, IEEE Open Journal of Vehicular Technology

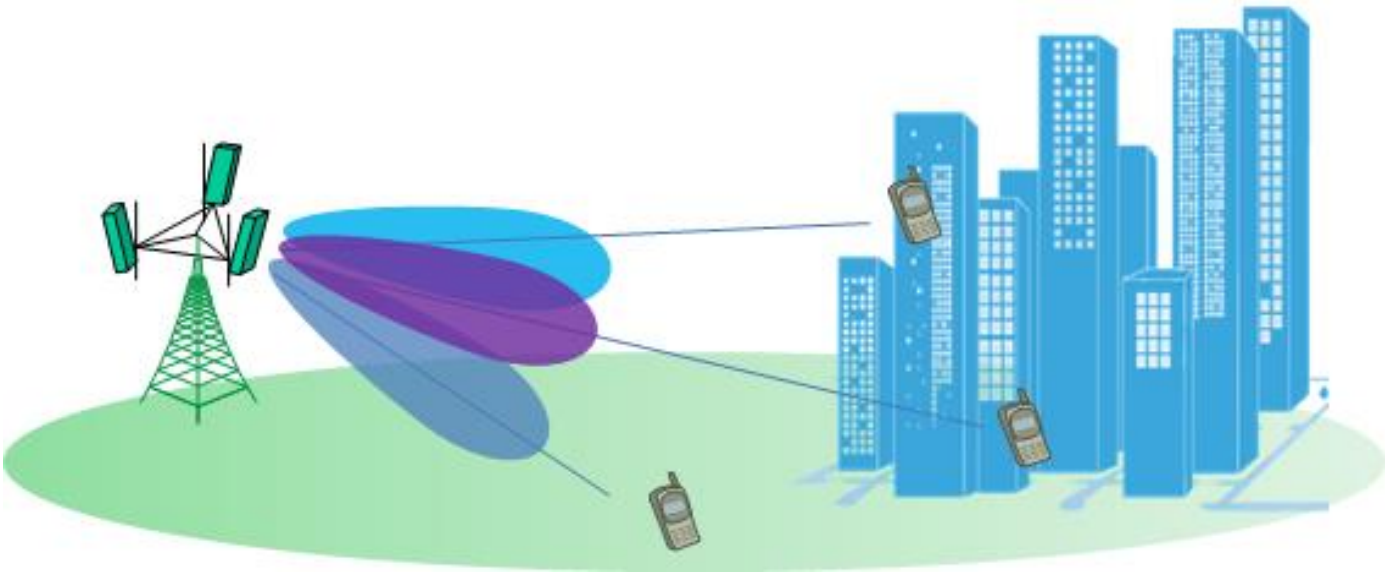

Fig. 1. 3D beamforming application scenario

Switched-beam systems [10] create fixed beam patterns. A decision has to be made as to which beams to choose at a given time based upon the demand of the system. On the contrary, the adaptive beamforming technique [11] synthesizes beams in arbitrary directions of interest while simultaneously nulling interfering signals in unintended angles of direction. Beamforming techniques have evolved from two-dimensional (2D) to three-dimensional (3D) beamforming not only covering horizontal, but also vertical such as is required for high-rise buildings. Like 2D beamforming, 3D beamforming may be developed based on switch-beam or adaptive beamforming.

2D beamforming employs a linear array antenna. Array elements of the linear array are aligned in a straight line separated from each other by equal or arbitrary length of distance measured in wavelength of carrier frequency. Due to the architectural limitation, a linear array can only form 2D beam pattern in either horizontal or vertical plane, thus it can only distinguish or separate users in different angles of either horizontal or vertical plane, lacking capability of identification in both planes at the same time. Therefore, 2D beamforming cannot make full use of 3D spatial domain [10]. While using the same principle as 2D beamforming, 3D beamforming can be implemented based on planar flat/volume array antennas, which has distinct characteristics in beam patterns. Contrary to 2D beamforming, 3D beamforming boasts capability of identifying users in full spatial dimension by forming 3D beam patterns in arbitrary cubic angle of directions, improving usage efficiency of spatial domain [11]. This is very important for combating the increasingly scarce resources in wireless communications.

3D beamforming technique is more attractive in massive MIMO wireless communications owning to the beneficial capability of controlling the strength of radiation field energy in different directions in spatial domain. Performances of 3D beamforming in wireless communications obviously relies on the properties of the beam pattern. Therefore, it is of importance to investigate in depth the properties and applications of 3D beamforming, analyzing system performance of massive MIMO communications, and evaluating the actual performance through field trials.

In this paper, we will analyze 3D beamforming properties and applications in wireless communications based on the physical structure of an array antenna, addressing the 3D beam pattern property of plane rectangular array antenna beamforming. We will present the closed-form formulae of antenna beam pattern parameters based on a rectangular array antenna. The field trials are carried out with 3D beamforming in a practical wireless communication scenario. The measurement results will be presented for single user and multiple users.

The rest of the paper is organized as follows. Section II introduces 3D beamforming application scenarios. Section III presents characteristics of the 2D beam pattern in a linear array. Section IV describes 3D beam patterns in a rectangular antenna array. Section V present the trial system and measurement results. Finally, Section VI concludes the paper.

II. 3D Beamforming Application Scenario

Due to ultra-high data rate transmissions, the coverage area of a 5G base station (BS), named next generation nodeB (gNB), should be much smaller than that of the 4G BS. In particular, in dense areas, where there are a number of high-rise buildings, the gNB must provide services through 3D beamforming. Figure 1 shows one application scenario, where there are high-rise buildings served by 5G massive MIMO, which provides 3D beams not only horizontally, but also vertically. Each vertical layer of the formed beams covers a number of floors in a high-rise building. Thus, in order to cover the whole high-rise building, multiple layers of beams are required.

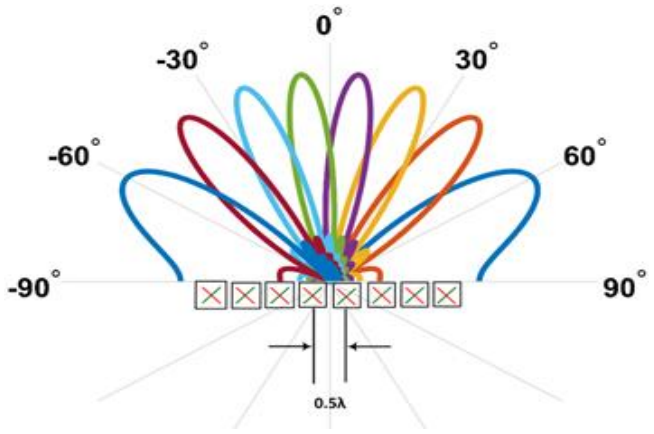

Fig. 2. Horizontal antenna array

III. Linear Arrays

First, we present the horizontal linear array. For each linear horizontal array, the spacing between two antenna elements is $d_h = 0.5\lambda$, where λ is the RF signal wavelength. N and θ represent the number of horizontal antenna elements and an angle of departure (AoD) at the horizontal plane. Assuming that each antenna element is weighted by a weighting factor, the normalized array factor of any horizontal beam n, where$n = 1,2,\cdots,N$, is given by [10]

$$A_n(\theta) = \frac{sin(\frac{d_h}{\lambda}\pi N \sin\theta - \beta_n)}{N sin(\frac{d_h}{\lambda}\pi \sin\theta - \frac{1}{N}\beta_n)} \quad (1)$$

where β_n is given by

$$\beta_n = \left(-\frac{N+1}{2} + n\right)\pi. \quad (2)$$

Fig. 2 shows the 8-antenna horizontal array with beamforming. It can be seen that N=8 beams are formed by the 8-antenna array. The effective angle range of horizontal coverage can be 120 degrees.

Second, we present the linear vertical array. In practice, the vertical angle of coverage should be smaller than the horizontal angle of coverage. Therefore, fewer layers of vertical beams may be considered. Assuming there are L vertical antenna elements with the space separation of 0.83λ between two adjacent elements. The L antenna elements are divided into M sub-arrays (equivalent units) with each sub-array consisting of L/M antenna elements. Note that each sub-array is weighted with one phase angle (one RF chain). Assuming that each sub-array has three antenna elements (i.e.L/M =3), the space separation between two equivalent units is $d_v = 0.83\lambda \cdot L/M = 0.83\lambda \cdot 3 = 2.49\lambda$. Assuming that ϕ represents an AoD at the vertical, the normalized array factor of any vertical beam m, $m = 1,2,\cdots,M$, is given by

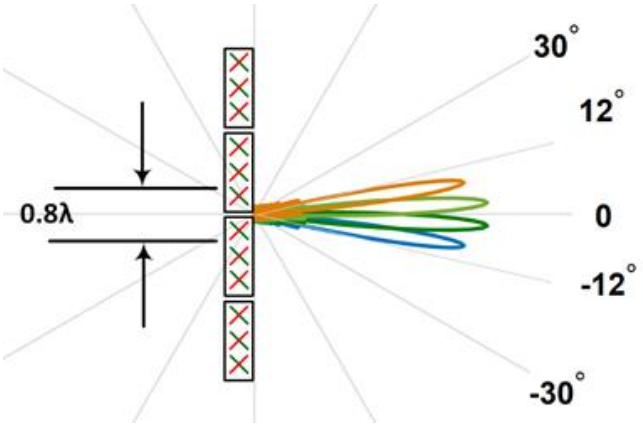

Fig. 3. Equivalent vertical antenna sub-arrays, four sub-arrays (4 RF chains) with 3 antenna elements in each sub-array.

$$B_m(\phi) = \frac{sin(\frac{d_v}{\lambda}\pi M \sin\phi - \beta_m)}{M sin(\frac{d_v}{\lambda}\pi \sin\phi - \frac{1}{M}\beta_m)} W_L(\phi) \quad (3)$$

where β_m is given by (2) with substitution of N and n with M and m, respectively, $W_L(\phi)$ is a window function depending on the number, L, of each equivalent element and given by [11]

$$W_L(\phi) = \left|\frac{sin(0.83\pi L \sin\phi)}{0.83\pi L \sin\phi}\right| \quad (4)$$

When L=1, $W_L(\phi) = 1$ for vertical AoD, which is a constant window function. Fig. 3 shows the beam patterns for M=4 and L=12. It can be seen that for four equivalent antenna units, the four vertical beams may cover 24-degree angles.

IV. Rectangular Antenna Arrays

The conceptual block diagram of the rectangular antenna arrays is shown in Figure 4. The rectangular antenna array structure has 32 antenna elements (4 rows and 8 columns). Since each sub-array has *3* vertical antenna elements, the rectangular array has 96 antenna elements in total. Each sub-array is connected to one dedicated RF chain, there are up to 32 RF chains.

When L/M=3, the space between two adjacent sub-arrays

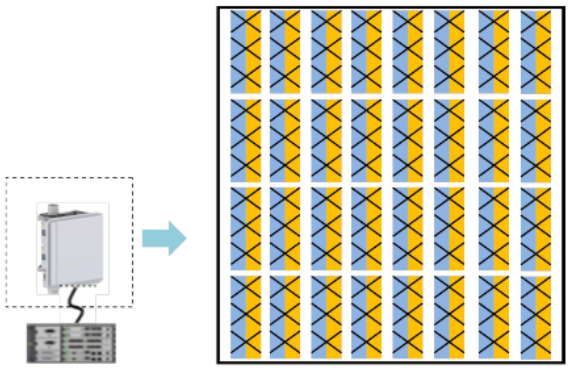

Fig. 4. Rectangular antenna configuration (4x8 sub-array configuration).

This article has been accepted for publication in a future issue of this journal, but has not been fully edited. Content may change prior to final publication. Citation information: DOI 10.1109/OJVT.2020.3030774, IEEE Open Journal of Vehicular Technology

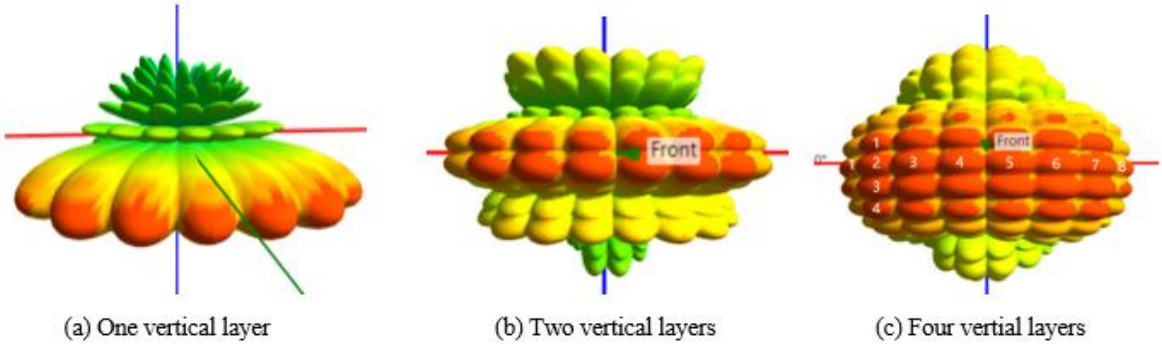

(a) One vertical layer (b) Two vertical layers (c) Four vertial layers

Fig. 5: Complete beam patterns, (a) one layer of vertical beams (1x8 sub-array configuration), (b): two layers of vertical beams (2x8 sub-array) configuration, (c) 4 layers of vertical beams (4x8 sub-array configuration)

is 2.4λ. By considering downlink digital beamforming similarly to the Butler method, 32 sub-arrays may form 32 beams with 4 rows (vertical) and 8 columns (horizontal). The normalized array factor of any 3D beam is given by

$$C_{nm} = A_n(\theta) \cdot B_m(\phi) \tag{5}$$

Fig. 5 illustrates the beam pattern generated according to (5). In the vertical plane, all the beams are within 24 degrees, while in the horizontal plane, all the beams are within 120 degrees (or, typically one sector). The vertical range of 24 degrees may cover most realistic scenarios for building coverage. If each beam supports one user, 32 users may be supported by this complete MIMO architecture. Further, if antenna polarization technology is used [11], each beam may support two users through the two polarizations, and the number of users may be doubled so that 64 users may be supported by only using the spatial domain.

V. Filed Trial Results

In this section, some representative field trial results are presented. Single and multiple users are considered. The field trials are specified as follows. In the urban area, a total of 30 or 60 gNBs are deployed, and the distance between two gNBs is around 450 to 500 meters. The main system parameters and specifications are listed in Table I.

A. RSRP comparison for multiple broadcast vertical beams in a building

In the trial system, each targeted building is covered by vertical multicast beams generated at an individual BS which is located at a height similar to the height of the building. The coverage method is different for different heights and locations of the buildings. (1) For a medium-rise building (e.g. below 75m) located near the middle point of the BS coverage area (abbreviated as midpoint), as demonstrated in Fig. 6, 2 or 4 beams are used to cover the building. The middle and high-levels of floors could be

TABLE I
Main System Parameters and Specifications

System Parameters	Specifications
System	5G new radio (NR) stand alone (SA) under 3GPP Rel-15 [16].
Bandwidth	100MHz at 2.6GHz
Subframe configuration	period of 5ms, DDDDDDDSUU, where D, S, and U stand for downlink subframe, special subframe, and uplink subframe, respectively.
Special subframe configuration:	DwPTS: GP: UpPTS = 6 symbols:4 symbols:4 symbols, where DwPTS GP and UpTPS indicate downlink pilot time slot, guard period and uplink pilot time slot, respectively.
Antenna configurations	base station 64T64R; terminal: 2T4R
Base station total transmit power	200W (53dBm)
Terminal transmit power	total 26dBm (23dBm per single antenna)
Multi-user scheduling algorithm	proportional fairness method (PF)

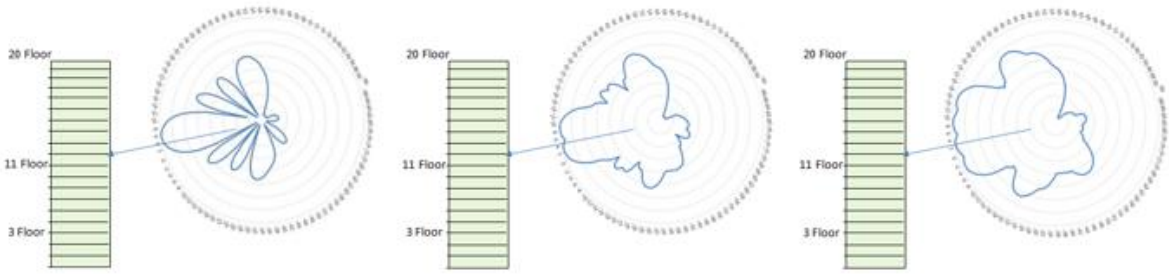

(a) One beam (b) Two beams (c) Four beams

Fig. 6: A medium-rise building covered by 1,2 or 4 vertical beams

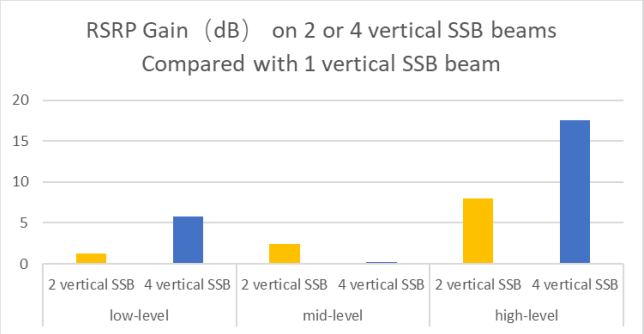

Fig. 7: RSRP comparison for different floor level in a medium-rise building.

covered by the main beam(s), and the reference signal received power (RSRP) indicated by the synchronisation signal block (SSB) is relatively high, about 1 ~ 17 dB, compared to single vertical beam; (2) For a large high-rise building (e.g. over 140m) near the midpoint, due to the limited dynamic range of the SSB scan, the upper floors are covered by the sidelobes of beams. The RSRP and SINR gains of the upper floors are reduced to about 2dB for 2 or 4 vertical beams, compared to single beam.

In order to demonstrate the impact of using multiple beams, a trial system was set up for a medium-rise building surrounded by multiple medium-rise and high-rise buildings in a dense urban area. The reference building with a height of 57 meters is 120 meters away from the BS. The BS has a height of 54 meters. Fig. 7. shows the impact of multi-beams on the RSRP gain, which is defined as the ratio of RSRP of 2 or 4 vertical SSB beams to that of 1 vertical SSB beam. It can be seen from Figure 7 that the vertical 2 or 4 SSB vertical coverage area is significantly larger than that of the single SSB in the lower and upper levels where the main lobe of the single SSB is not aligned. It is shown that the maximum gain of 2 SSB RSRP is 8 dB, while the maximum gain of 4 SSB RSRP is 17dB.

B. Performance of Single and Multiple Users in Case of 2D Beamforming

In this section, the data rate for both downlink (DL) and uplink (UL) transmissions is demonstrated when a single user and multiple users are located on the horizontal plane in case of 2D beamforming.

1) Single User

In the trial of the single user performance, SA outdoor

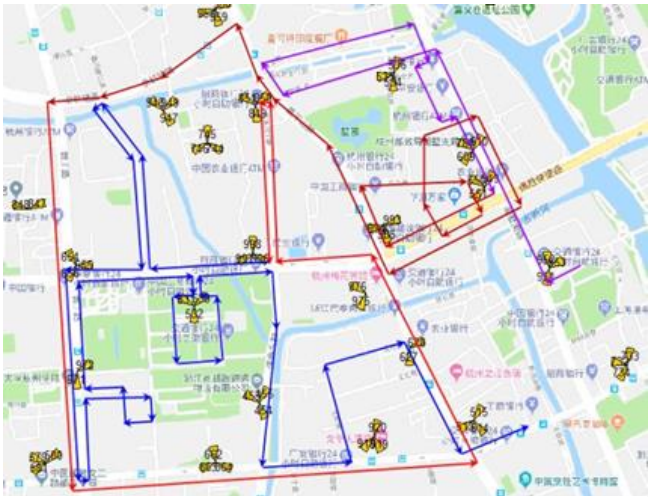

Fig. 8. Single-user trial roadmap

road traversal tests were carried out and the measured throughputs of the mobile terminal were recorded. The trial roadmap is shown in Fig. 8, where the different colors shows different moving routes. In the trial, with a moving speed of around 30km/h, the testing mobile device was moving in a field covered by 20 BSs, including about 60 small cellular sectors. The distance between any two BSs is about 350 meters to 400 meters. When the testing mobile device was located in the coverage area of one cellular sector, it was served with the full resources of this sector. At the same time, other sectors in the trial area added up to 50% load as interference. That is, the full transmit power of each BS was used to add up to 50% physical resource blocks (PRBs) or orthogonal channel noise generation (OCNG). The traffic load from other sectors caused interference to the testing mobile device.

Table II lists the downstream number and rate in outdoor traversal test, while Table III lists the upstream number and rate in outdoor traversal test. It can be seen from the two tables that when the neighboring zone is unloaded, the ratio of downlink four streams is about 10%, the ratio of downstream three streams is about 67%, and the average downlink data rate can reach up to 900Mbps; the ratio of uplink dual streams can reach 100%, and the average uplink data rate can reach about 109Mbps. Under the loading condition of 50% downlink in the neighboring area, due to increased interference, the ratio of large streams decreases, the ratio of downlink three-streams drops to 44%, the ratio

TABLE II

MAIN SYSTEM PARAMETERS AND SPECIFICATIONS

	DL Rank 1&2 ratio	DL Rank 3 ratio	DL Rank 4 ratio	DL user data rate(Mbps)
Neighbor cells 0% loaded	22%	67%	11%	895
Neighbor cells 50% loaded	56%	44%	0%	483

TABLE III

UPSTREAM NUMBER AND RATE IN OUTDOOR TRAVERSAL TEST

	UL Rank 2 ratio	UL user data rate(Mbps)
Neighbor cells 0% loaded	100%	109

This article has been accepted for publication in a future issue of this journal, but has not been fully edited. Content may change prior to final publication. Citation information: DOI 10.1109/OJVT.2020.3030774, IEEE Open Journal of Vehicular Technology

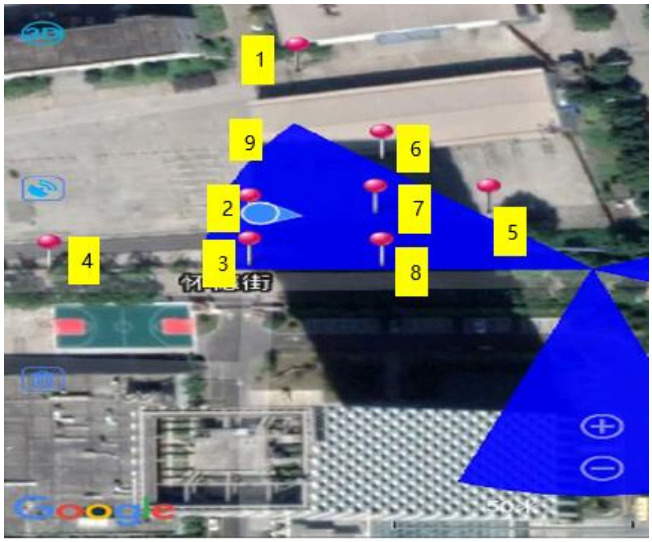

Fig. 9: Multiple (less than or equal to 10 users) trial site.

of downlink four-streams drops to 0, and the average downlink data rate drops by 30% -40% to 483Mbps

2) 1 to 9 Users

In order to investigate the performance of cell throughput and stream number adaptively changing with the number of users, first we conducted the following tests: 1, 3, 5, 7, 8, and 9 users, respectively, being served simultaneously, and recorded the cell throughput. The precoding technology of minimum mean square error (MMSE) was used for the multiuser communications. Fig. 9 shows the multiuser trial site. Data streams were transmitted at the same time for three minutes for a varying number of users. The cell throughputs of 1/3/5/7/8/9 users, respectively, were measured.

Fig. 10 shows the testing peak throughputs for 1/3/5/7/8/9 users, where all users were located at good points in absence of adjacent cell interference. In order to better ensure the effect of pairing [11], in the multi-user pairing process, the number of streams for each user is 2 downstreams and 1 upstream. It can be seen from the figure that when the number of users is small, increasing the number of users increases the peak throughput for both DL and UL. When there are 8 users, corresponding to 8 horizontal beams, the maximum number of streams in the cell is reached (16 streams downstream, 8 streams upstream); when the number of terminals (i.e. users) continues to increase beyond 8, the cell throughput will be relatively stable.

Through using the 64T64R base station equipment, the service beam is narrower and the number of layers is larger. With a 2T4R terminal, the maximum number of downlink streams for a single user is 4 and the maximum number of uplink streams is 2; while the typical maximum number of downlink streams in a cell can reach up to 16 and the typical maximum number of uplink streams can reach up to 8. Theoretically, this is about 4 times the peak rate of a single user. The peak throughput of the cell under multiple users is determined by the maximum processing capacity of the network, and its performance is closely related to the algorithm of 5G key large-scale antenna technology [11]. When there is enough space separation or beam isolation between multiple users and the signal is good, the peak throughput of the cell can be reached. In the trial, the measured peak throughput of the cell is about 3 times the peak throughput of a single user, and the downlink and uplink can reach more than 5Gbps and 650Mbps, respectively.

In practice, the distribution of users is random, which cannot ensure good separation between different users. At this time, the average cell throughput should be smaller and the peak throughput of the cell will be reduced. The main factors impacting the average cell throughput include user random distribution and moving speed. Assume 10 users in the field testing of average cell throughput. Figures 11 and 12 illustrate the downlink and uplink cell throughputs, in which 4 cases are considered: (1) all users are located at good points, in absence of adjacent cell interference, (2) Evenly static distribution, where 1/2/3/4 users are located at excellent/good/fair/bad points, respectively, in presence of 50% adjacent cell interference; (3) Concentrated static distribution where the separation of users should be less than 1 meter in presence of 50% adjacent cell interference; (4) evenly moving distribution in presence of 50% adjacent cell interference. Of the 10 users, 4 users slowly move among excellent/good/fair/bad points, 4 users move at the speed of 3km/h between good and bad points, 2 users move

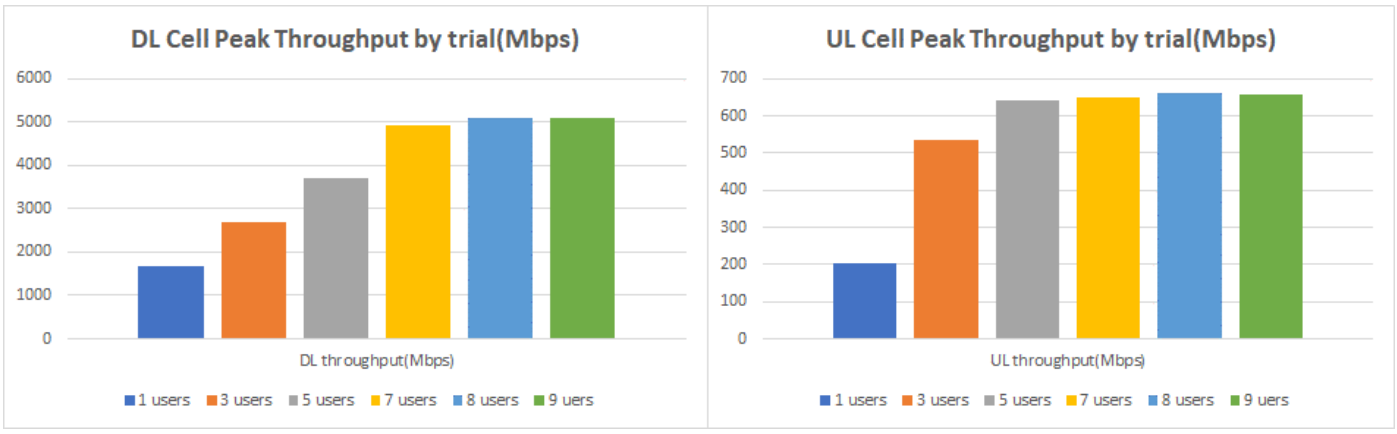

Fig. 10. Cell throughput when the number of users is 1, 3, 5, 7, 8, 9 respectively.

This article has been accepted for publication in a future issue of this journal, but has not been fully edited. Content may change prior to final publication. Citation information: DOI 10.1109/OJVT.2020.3030774, IEEE Open Journal of Vehicular Technology

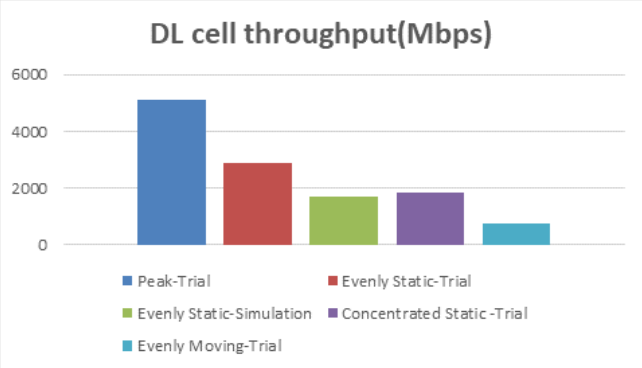

Fig. 11: Impact of user distribution and mobility on downlink cell throughput.

at a fast speed of 60km/h between good and bad points. It can be seen from the figures that in the centralized distribution of users relative to even distribution, the impact of spatial separation between users becomes worse, so that the performance of multi-user pairing degrades, and the average throughput of the cell decreases by 35% to 50% for DL and UL, respectively. In a multi-user moving scenario, since the channel information between different users varies greatly, the accuracy of channel state information (CSI) estimation degrades, the rate is 50% -70% lower than that of the fixed-point even distribution.

In order to show some performance comparison between trial and simulation results, the multiuser simulation has been carried out specifically by considering case (2): the evenly static scenario. The simulation results in case (2) have been added in Fig. 11 and Fig. 12. It can be seen from the figures that the simulated cell throughputs are 1.71Gbps, and 288Mbps for downlink and uplink, respectively, whereas the trial cell throughputs are 2.88Gbps, and 482Mbps for downlink and uplink, respectively. Therefore, the trial results are higher than simulation results. The main reason is that in the actual trial, the locations of the user distribution have specially been selected in the way that different users are located in different beams so that the number of pairing data streams among multiple users is relatively high.

3) Larger Than 10 Users

In order to further verify the network performance in large-

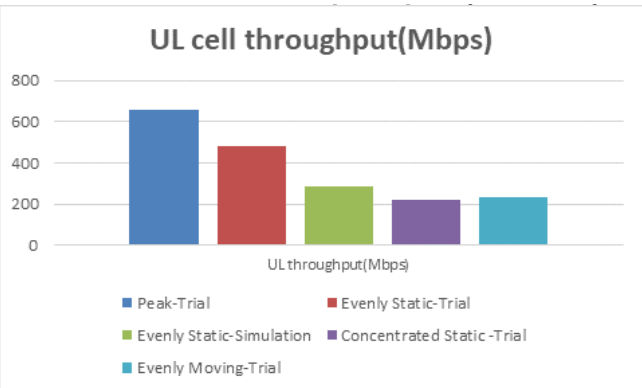

Fig.12: Impact of user distribution and mobility on uplink cell throughput.

40 users, 60 users, 80 users, 100 users gradually, and repeat

Fig.13. Multiuser (larger than 10 users) trial site

the above steps. All the users are located at the premeasured and selected good points of the signal and are distributed as uniformly as possible within each service beam of the base station. The measured downlink cell throughput is 4.2Gbps-4.5Gbps, and the uplink cell throughput is about 450Mbps-480Mbps. When increasing from 20 users to 100 users, due to increased interference between multi-user streams, the average throughput of the uplink and downlink is reduced slightly by 5% to 10% as shown in Fig. 14.

C. Performance of Single User in Case of 3D Beamforming

In order to evaluate the coverage performance of 3D beamforming with 2/4 vertical beams, we consider the simple scenario of single user. The test building is located at about 120 meters away with height of 57 meters from the

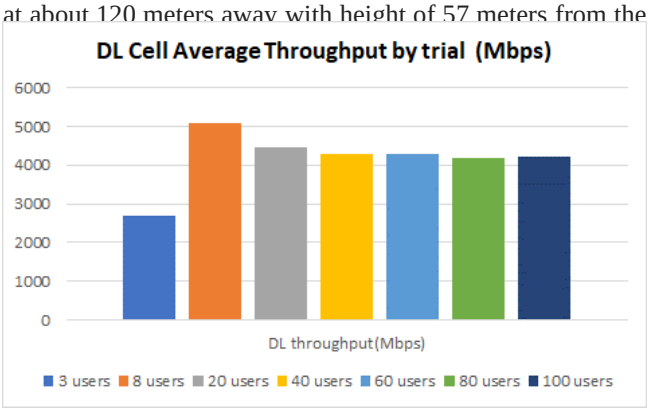

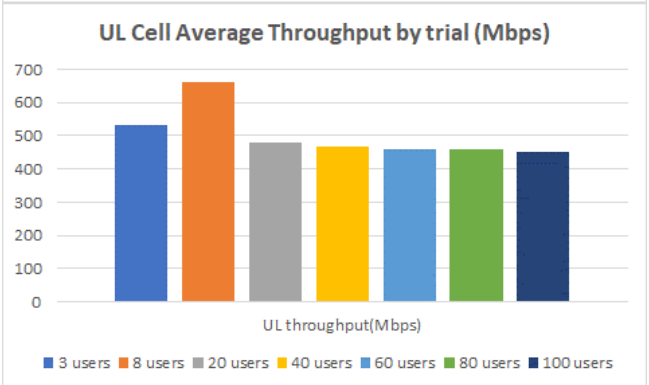

Fig. 14: Impact of the number of users on cell throughput in large-capacity scenario

This article has been accepted for publication in a future issue of this journal, but has not been fully edited. Content may change prior to final publication. Citation information: DOI 10.1109/OJVT.2020.3030774, IEEE Open Journal of Vehicular Technology

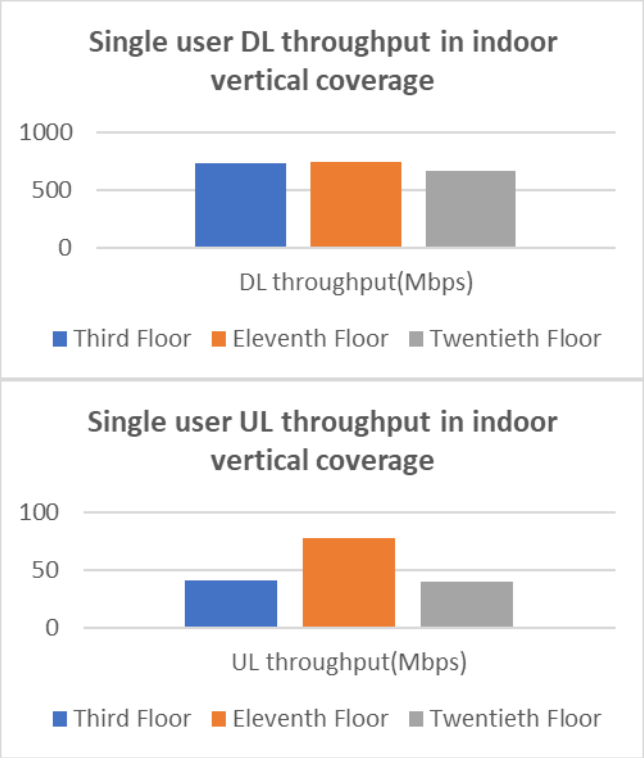

Fig. 15: Throughput of single user in case of 3D beamforming

5G gNB, which is 54 meters high. Therefore, the building is located in the straight direction of the 5G gNB sector. The building has a total of 20 floors. For testing, the single user is located on Floors 3, 11, and 20 as low, medium, and high floors, respectively. The average throughput over 2/4 vertical beams is shown in Fig. 15. It can be seen from the figure that because the dynamic range of the dimensional beam is increased, and the coverage performance of the vertical dimension is enhanced. For a typical building with a medium distance from the gNB, good coverage performance can be achieved in all the low, medium, and high-rise floors. Specifically, the DL rates of about 660-750Mbps and DL rates of around 40-78Mbps are obtained.

VI. Conclusion

In this paper, 3D beamforming of 5G massive MIMO systems has been studied to cover high-rise buildings. The field trial and measurement results have been presented in the cases of single and multiple mobile users. From the field trial results, the following conclusions have been drawn:

(1) The multilayer beams from 64 transmit/receive antennas at a base station (gNB) can cover high-rise buildings with a height of 140 meters with good receive signal quality.

(2) For 2D beamforming, in the case of single user with 4 receive antennas, 3 and 4 data streams can be accommodated with 67% and 10% respectively. However, if a neighbour cell is 50% loaded, the 3 and 4 streams may be supported with 44% and 0%, respectively, so that the data rate is reduced significantly due to intercell interference.

(3) For 2D beamforming, in the case of a number of users, the total sum rate from all users can be increased multiple times (i.e. 3 to 4 times) as large as that of a single user. When the number of users is larger than 8, the sum rate has been saturated.

(4) Users with uniform distribution can achieve larger sum rate than users with centralized distribution due to space separation.

(5) Under static user conditions, the performance of the multi-antenna system is the best; under low-speed mobile conditions, the performance of the multi-antenna system drops sharply, even by more than 50%.

(6) For 3D beamforming, in a typical building with a medium distance from the gNB, good coverage performance can be achieved in all the low, medium, and high-rise floors.

Acknowledgment

This 5G research work has been carried out through twin-project collaboration between European Union and China. The authors would like to thank the funding support by the EU Horizon 2020 Research and Innovation Programme, grant agreement no: 814956 (5G-DRIVE) and the China 2018 New Generation Broadband Communication Mobile Communication Major Special Project "5G Product Research and Development Scale Test"（2018ZX03001022).

References

[1] D. Wang, M. Wang, P. Zhu, J. Li, J. Wang, and X. You, “Performance of network-assisted full-duplex for cell-free massive MIMO,” IEEE Transactions on Communications, vol. 68, no. 3, pp. 1464-1478, Mar. 2020.

[2] H. Wei, D. Wang, H. Zhu, J. Wang, S. Sun, and X. H. You, “Mutual coupling calibration for multiuser massive MIMO systems,” *IEEE Transactions on Wireless Communications*., vol. 15, no. 1, pp. 606-619, Jan. 2016.

[3] C. Pan, H. Zhu, N. J. Gomes, and J. Wang, "Joint Precoding and RRH selection for User-centric Green MIMO C-RAN," *IEEE Transactions on Wireless Communications*., vol. 16, no. 5, pp. 2891-2906, May 2017.

[4] J. Wang, H. Zhu, and N. Gomes, “Distributed antenna systems for mobile communications in high speed trains,” *IEEE Journal on Selected Areas in Communications*., vol. 30, no. 4, pp. 675-683, May 2012.

[5] H. Zhu, “Performance comparison between distributed antenna and microcellular systems,” *IEEE Journal on Selected Areas in Communications*, vol. 29, no. 6, pp. 1151-1163, 2011.

[6] H. Zhu and J. Wang, “Radio resource allocation in multiuser distributed antenna systems,” *IEEE Journal on Selected Areas in Communications*., vol. 31, no. 10, pp. 2058-2066, Oct. 2013.

[7] W. Xu, “Capacity improvement analysis of 3D-beamforming in small cell systems,” *Science China Information Sciences*, vol . 61, February 2018.

[8] S Chen, S Sun, G Xu, X Su, and Y Cai, “Beam-space multiplexing: practice, theory, and trends-from 4G TD-LTE, 5G, to 6G and beyond,” *IEEE Wireless Communications*, vol. 27, no. 2, pp.162-172 , Apr. 2020.

[9] S Chen, Y-C Liang, S Sun, S Kang, W Cheng, and M. Peng, “Vision, requirements, and technology trend of 6G: how to tackle the challenges of system coverage, capacity, user data-rate and

movement speed," *IEEE Wireless Communications*, vol. 27, no. 2, pp. 218-228, Apr. 2020.

[10] J. Wang, H. Zhu, L. Dai, N. J. Gomes, and J. Wang, "Low-complexity beam allocation for switched-beam based multiuser massive MIMO systems," *IEEE Transactions on Wireless Communications*, vol. 15, no. 12, pp. 8236-8248, Dec. 2016.

[11] Kuang and W Deng, "5G Massive MIMO technology and effect to networking and optimization", *China Mobile Communications*, vol 43, August 2019.

[12] M. Sakai et al., "Experimental Field Trials on MU-MIMO Transmissions for High SHF Wide-Band Massive MIMO in 5G," IEEE Transactions on Wireless Communications, vol. 19, no. 4, pp. 2196-2207, April 2020.

[13] K. Yamazaki et al., "DL MU-MIMO Field Trial with 5G Low SHF Band Massive MIMO Antenna," 2017 IEEE 85th Vehicular Technology Conference (VTC Spring), Sydney, NSW, 2017, pp. 1-5.

[14] T. Kashima et al., "Large scale massive MIMO field trial for 5G mobile communications system," 2016 International Symposium on Antennas and Propagation (ISAP), Okinawa, 2016, pp. 602-603.

[15] G. Liu, X. Hou, J. Jin, F. Wang, Q. Wang, Y. Hao, Y. Huang, X. Wang, X. Xiao, and A. Deng, "3-D-MIMO with massive antennas paves the way to 5G enhanced mobile broadband: from system design to field trials," IEEE Journal on Selected Areas in Communications, vol. 35, pp. 1222-1233, no. 6, June 2017.

[16] 3GPP Release 15, https://www.3gpp.org/release-15

Jiangzhou Wang (Fellow, IEEE) is currently a Professor and the former Head of the School of Engineering and Digital Arts, University of Kent, U.K. He has published over 300 papers and 4 books in the areas of wireless communications. Professor Wang is a Fellow of the Royal Academy of Engineering, U.K., Fellow of the IEEE, and Fellow of the IET. He was a recipient of the Best Paper Award from the IEEE GLOBECOM2012. He was an IEEE Distinguished Lecturer from 2013 to 2014. He was the Technical Program Chair of the 2019 IEEE International Conference on Communications (ICC2019), Shanghai, the Executive Chair of the IEEE ICC2015, London, and the Technical Program Chair of the IEEE WCNC2013. He has served as an Editor for a number of international journals, including IEEE Transactions on Communications from 1998 to 2013.

Wei Deng is Deputy Director of China Mobile Research Institute (CMRI) Wireless and Terminal Department, responsible for China Mobile 5G commercial strategy and technical work. He received Master degree in Signal and Information system from Beijing University of Posts and telecommunications in 2004, and his major research direction is cellular mobile communication.

Xin Li received Master of Science (M.S.) in Communication & Information System from Beijing University of Posts and Telecommunications (BUPT), Beijing, China., in 2002.From 2002 to now, he has been working in China Mobile Research Institute. He is responsible for wireless communication networking techniques research and filed test in 3G,4G, NB-IoT and 5G.

Huiling Zhu (SM'17) received the B.S degree from Xidian University, Xi'an, China, and the Ph.D. degree from Tsinghua University, Beijing, China. She is currently a Reader (Associate Professor) in the School of Engineering and Digital Arts, University of Kent, Canterbury, United Kingdom. Her research interests are in the area of wireless communications, covering topics such as radio resource management, MIMO, cooperative communications, device-to-device communications, Cloud RAN, and Fog RAN. She received the best paper award from IEEE Globecom 2011, Houston. She has participated in a number of European and industrial projects in these topics and was holding European Commission Marie Curie Fellowship from 2014 to 2016. She has served as the Publication Chair for IEEE WCNC 2013, Operation Chair for IEEE ICC 2015, Symposium Co-Chair for IEEE Globecom 2015 and IEEE ICC 2018, and Track Co-Chair of IEEE VTC2016-Spring and VTC2018-Spring. Currently, she serves as an Editor for IEEE Transactions on Vehicular Technology.

Manish Nair received the B.E. degree in electronics and communications engineering from Vivesvaraya Technological University (VTU), India, in 2007, M.S. degree in electrical engineering from The University of Texas at Dallas (UTD), in 2010 and Ph.D. degree in Electronic Engineering from the University of Kent in 2019. From 2009 to 2014, he was associated with Nokia Siemens Networks, Skyworks Solutions Inc., Samsung Telecommunications America, and Qualcomm in RF power amplifier design, RF standards, RF systems and RF applications engineering capacities. He is now an Honorary Research Associate at the University of Kent and a Senior Research Associate at the University of Bristol. He currently serves as a Technical Program Committee (TPC) Member in IEEE Wireless Communication and Networking Conference (WCNC) and IEEE International Communications Conference (ICC).

Dr. Tao Chen is a senior researcher at VTT Technical Research Centre of Finland, the honorary professor at University of Kent, and the adjunct professor at University of Jyväskylä. He has more than 20 years of experience in the telecommunications sector. He has led several EU and national research projects, covering the topics from cognitive radio, green communications, to software defined networking and 5G radio access networks. Dr. Chen is technical editor of IEEE Wireless Communications Magazine and IEEE Transactions on Cognitive Communications and Networking. He has published more than 70 scientific publications. His current research interests include software defined networking for 5G mobile networks, massive IoT in 5G, dynamic spectrum access, AI for communications, energy efficiency and resource management in heterogeneous wireless networks.

This article has been accepted for publication in a future issue of this journal, but has not been fully edited. Content may change prior to final publication. Citation information: DOI 10.1109/OJVT.2020.3030774, IEEE Open Journal of Vehicular Technology

Na Yi (M'10) received the Ph.D. degree in wireless communications from the University of Surrey, U.K., in 2009. She joined the Institute for Communication Systems (ICS), University of Surrey, Surrey, UK in 2009, where she is currently a Senior Research Fellow. Her current research interests and expertise cover THz communications, cognitive radios/networks, advanced signal processing in wireless communications and sensor networks, cooperation and relaying in wireless networks, and cognitive resource allocation for wireless networks.

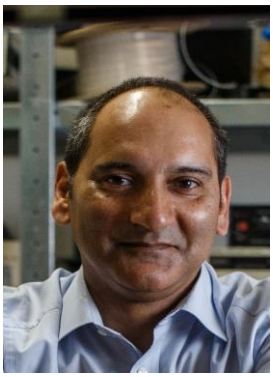

Nathan J. Gomes (M'92–SM'06) received the B.Sc. degree in electronic engineering from the University of Sussex, Sussex, U.K., in 1984, and the Ph.D. degree in electronic engineering from University College London, London, U.K., in 1988.

From 1988 to 1989, he was a Royal Society European Exchange Fellow with ENST, Paris, France. Until 2020, he was with the University of Kent, Canterbury, U.K., and was Professor of Optical Fiber Communications. He is now an Honorary Professor at the University of Kent, and a Professorial Teaching Fellow at University College London. His current research interests include fiber-wireless access systems and networks, fronthaul, and radio-over-fiber technology. He was the TPC Chair of the IEEE International Conference on Communications (ICC 2015), London.